

STATISTICS OF QUASIENERGIES IN CHAOTIC AND RANDOM SYSTEMS

Mario FEINGOLD* and Shmuel FISHMAN

Department of Physics, Technion-Israel Institute of Technology, 32000 Haifa, Israel

Received 31 March 1986

The statistics of quasienergies are analyzed for periodically driven chaotic systems and found to be similar to those of truly random models. These differ from the results that were obtained so far, for chaotic systems with time-independent Hamiltonians. The separations of the quasienergies and the Δ_3 -statistic are calculated numerically for chaotic, as well as for truly random models. Local statistical measures are introduced in order to investigate the repulsion of quasienergies. The results provide further evidence for Anderson localization in chaotic systems with Hamiltonians that are periodic in time.

1. Introduction

The theory of statistics of random matrices that was developed by Wigner, Dyson and their successors [1] was applied extensively to the analysis of spectra of complicated systems. Wigner argued that statistical properties of spectra of complicated Hamiltonians are similar to those of random ones. Therefore, for such systems the Hamiltonian matrices can be taken from an ensemble of random matrices with symmetries similar to those of the exact Hamiltonian. In such a description we ignore many details of a particular system such as the detailed interactions. We obtain a simple statistical description of general properties or large families of systems. In some sense it is similar to the general framework of statistical mechanics. Random matrix theory was very successful for the description of the spectra of many complicated systems such as nuclei [2], atoms [3] and molecules [4]. For Hamiltonians with no additional symmetries the random matrices belong to the Gaussian unitary ensemble (GUE). The elements of these Hermitian matrices satisfy a Gaussian distribution and are statistically independent with the requirement that their

probability distribution is invariant under unitary transformations. If the Hamiltonian satisfies time reversal symmetry and is therefore a real symmetric matrix, it belongs to the Gaussian orthogonal ensemble (GOE). Within this ensemble the probability distribution is invariant under orthogonal transformations. A statistical property that is extensively studied is the distribution $P(s)$ of the neighboring level separations. For the GOE one finds the Wigner distribution [1, 2]

$$P(s) = \frac{\pi s}{2D^2} \exp\left[-\frac{\pi s^2}{4D^2}\right], \quad (1.1)$$

where D is the mean level spacing. The main feature of this distribution is the Wigner repulsion, namely the fact that the probability density $P(s)$, to find two neighboring levels with the spacing s vanishes for small s . For the GOE it vanishes linearly in s while for GUE it behaves as s^2 for small s . If the various eigenvalues of a matrix are totally uncorrelated the separations satisfy a Poisson distribution, namely,

$$P(s) = \frac{1}{D} e^{-s/D}. \quad (1.2)$$

The levels do not repel, and for small separations between neighboring levels (s) their probability density approaches the constant value $1/D$. This is the Poissonian ensemble (PE). Another statisti-

*The James Franck Institute, University of Chicago, IL 60637, USA.

cal measure that is extensively used is the Δ_3 -statistic [5, 2, 1]

$$\Delta_3(r) = \left\langle \min_{A, B} \frac{1}{2L} \int_0^{2L} [N(E) - AE - B]^2 dE \right\rangle, \quad (1.3)$$

where $r = 2L/D$ is approximately the mean number of energies, the brackets $\langle \rangle$ denote the ensemble average of energies, while $N(E)$ is the integrated density of states, namely,

$$N(E) = \sum_i \theta(E - E_i). \quad (1.4)$$

Therefore, Δ_3 measures the fluctuations in the density of states. For the GOE

$$\Delta_3(r) = \frac{1}{\pi^2} [\ln r - 0.0687], \quad (1.5)$$

while for the PE

$$\Delta_3(r) = r/15. \quad (1.6)$$

For classical systems very complicated motion may be generated by simple equations of motion [6, 7]. For Hamiltonian systems it is interesting to investigate how the classical chaotic nature is reflected in the behavior of the corresponding quantum-mechanical systems [8, 9]. It was predicted [10–12] that for chaotic systems with time-independent Hamiltonians Wigner repulsion takes place. These predictions were confirmed by numerical solutions for a variety of systems [13–14]. In particular the energy statistics satisfy (1.1) and (1.5). It was also established that the elements of the Hamiltonian matrix [15] and the wave functions are randomly distributed [16] for some model systems. For generic integrable systems it is expected [12] and found that there is no level repulsion and the levels satisfy a Poisson distribution. The level repulsion increases with the stochasticity parameter, namely, the parameter that controls what fraction of phase space is chaotic [14]. A crossover between Wigner and Poisson statistics in such systems is found. The

resulting distribution can be obtained in the semiclassical limit from a superposition of contributions from chaotic and regular regions in phase space [17]. For systems with time-independent Hamiltonians these statistical characterizations are valid only in the semiclassical regime. A given sequence of energies will exhibit deviations from the ideal statistical distribution due to the finite value of Planck's constant \hbar . In particular for the level separations of the rectangular well [18] one finds deviations from (1.2). It is found also that $\Delta_3(r)$ satisfies (1.6) only for $r < r^*$ while it saturates at a constant value for large r . It was pointed out by one of us [19] that when the energy increases and one approaches the semiclassical limit, the deviations of the distribution of the level separations from (1.2) decrease and r^* increases. In a very instructive paper Berry [20] proved that r^* is determined by the shortest classical orbits. The crossover point r^* is proportional to $\hbar^{-(\eta-1)}$ for integrable systems with η degrees of freedom, and to $\ln \hbar^{-1}$ for chaotic systems.

In this paper we will analyze a similar problem for chaotic systems with time-dependent Hamiltonians. In particular for periodically driven systems the quasienergies, rather than the energies are the good quantum numbers. In this work their statistics will be studied. The analysis will be performed in the framework of the kicked rotor model that is defined by the Hamiltonian

$$\mathcal{H} = \frac{\hbar^2}{2I} p^2 + \hat{k} V(\theta) \sum_n \delta(t - n), \quad (1.7)$$

where $p = -i\partial/\partial\theta$ is the angular momentum operator and I is the moment of inertia. The most natural choice of the driving potential is

$$V(\theta) = \cos \theta. \quad (1.8)$$

With this choice (1.7) generates the classical standard map that exhibits chaotic behavior [7, 21]. The stochasticity parameter is proportional to \hat{k} . The size of chaotic regions in phase space increases with \hat{k} and diffusion starts at some

critical value. The quantum mechanical behavior generated by (1.7) and (1.8) is found to be very different from the classical one [22–25]. In particular the diffusion in phase space is suppressed and the motion is quasiperiodic [23, 24]. It was shown [25] that the mechanism of this suppression is similar to Anderson localization [26]. Consequently the quasienergy states are exponentially localized in the same way electronic states are localized in disordered solids.

In an earlier paper [27] we analyzed the distribution of separations of quasienergies of the kicked rotor that is defined by (1.7) and (1.8). We concluded that this distribution is Poissonian, namely (1.2). It is similar to the corresponding distribution of the energies of localized electronic states in disordered solids [28], and supports the correspondence between these problems [25]. This distribution is very different from the one obtained for time independent chaotic systems [10–14]. We found that quasienergy states that are localized on momentum states with separations that are smaller than the localization length repel and satisfy a distribution similar to (1.1). Recently Izrailev [29] studied a model, that is similar to some extent to the kicked rotor [(1.7)–(1.8)] for strongly overlapping quasienergies. These results are consistent with ours. In his work he studied the effect of changes in the symmetry on the nature of repulsion, namely on the power of the probability density for small separations.

In the present paper the analysis of the quasienergy separations will be extended to another pseudorandom model and to the corresponding truly random models. The statistic Δ_3 will be calculated for all these models. The main purpose of the paper is to compare various statistical properties of the quasienergies of classically chaotic or pseudorandom models defined by (1.7) with those of the corresponding truly random models. The outline of the paper is as follows: in section 2 the various models will be defined, the various distributions of separations will be analyzed in section 3 and the statistic Δ_3 will be calculated in section 4. The conclusions are summarized in section 5.

2. Models

The models that will be investigated in this work are generated by the Hamiltonian (1.7) that describes a periodically kicked rotor. The wavefunction ψ just before the $(n + 1)$ th kick is related to the one before the n th kick via

$$\psi(\theta, n + 1) = T\psi(\theta, n). \quad (2.1)$$

The evolution operator is

$$T = \exp[-i\tau p^2/2] \exp[-ikV(\theta)], \quad (2.2)$$

where $\tau = \hbar/I$ and $k = \hat{k}/\hbar$. The form (2.2) is obtained by formal integration of the Schrödinger equation with the Hamiltonian (1.7). The quasienergy states are the eigenstates of T , namely,

$$T\psi_\omega(\theta, t) = \Lambda_\omega\psi_\omega(\theta, t), \quad (2.3)$$

where $\Lambda_\omega = e^{-i\omega}$ and ω is the quasienergy. Since T is unitary ω is real. The eigenstates take the form

$$\psi_\omega(\theta, t) = e^{-i\omega t}u_\omega(\theta, t). \quad (2.4)$$

It was shown [25] that the quasienergies satisfy the equation

$$T_m u_m + \sum_r W_r u_{m+r} = E u_m, \quad (2.5)$$

with $u_m = \frac{1}{2}(u_m^+ + u_m^-)$, where u_m^- and u_m^+ are the projections of u_ω on the angular momentum state m , just before and after a kick respectively. The W_r are the Fourier components of

$$W(\theta) = -\tan\left[\frac{k}{2}V(\theta)\right], \quad (2.6)$$

with the definition $E = -W_0$, while

$$T_m = \tan\left[\frac{1}{2}(\omega - \frac{1}{2}\tau m^2)\right]. \quad (2.7)$$

It was argued that if τ is an irrational multiple of π the sequence $\{T_m\}$ can be considered pseudorandom. If $\{T_m\}$ is random (2.5) is just a one-

dimensional Anderson model for localization with diagonal disorder. If the hopping matrix elements W_r fall off sufficiently fast with r , all the states are exponentially localized.

For the most natural driving $V(\theta) = \cos \theta$ (eq. 1.8) the W_r fall off exponentially only for $k < \pi$. Numerical calculations indicate, however, that the quasienergy states are localized also for $k > \pi$. Recently Shepelyansky [30] reformulated (2.5) so that the hopping is of short range, namely,

$$\sum_r J_r(k/2) \sin \frac{1}{2}(\omega - \frac{1}{2}\tau m^2 - \pi r) \tilde{u}_{m+r} = 0, \quad (2.8)$$

where \tilde{u}_r are the Fourier components of $\tilde{u}_\omega(\theta) = u^-(\theta) \exp[-\frac{1}{2}k \cos \theta]$ and J_r are the Bessel functions of the first kind. Even if all phases $\frac{1}{2}\tau m^2$ can be considered random (2.8) is an unexplored Anderson model with correlations between diagonal and off-diagonal randomness. In what follows this type of kicked rotor, defined by (1.7) and (1.8) will be called model C [since $V(\theta) = \cos \theta$].

For a transparent comparison with localization theory it is useful [25] to define a model, that will be called model A, in what follows,

$$V(\theta) = -\frac{2}{k} \arctan(k \cos \theta - E). \quad (2.9)$$

In all the calculations we will take $E = 0$. The resulting hopping in the corresponding Anderson model (2.5) is to nearest neighbors only, namely,

$$W_r = \frac{1}{2}k \delta_{|r|,1}. \quad (2.10)$$

Moreover, if the argument of the tangent in (2.7) can be considered random this is just the Lloyd model for localization [31] where the localization length ξ is known analytically [32, 33] and satisfies

$$2k \cosh \gamma = \left[(E - k)^2 + 1 \right]^{1/2} + \left[(E + k)^2 + 1 \right]^{1/2}, \quad (2.11)$$

where $\gamma = 1/\xi$. It was confirmed that model A has the same localization length as the corresponding random model [25].

Since the quasienergies are localized on angular momentum states there is a preferred representation of T . The matrix elements of the evolution operator T of (2.2) for model C in the angular momentum representation are

$$T_{mr}^C = \exp(-i\tau m^2/2) \cdot (-i)^{|m-r|} J_{|m-r|}(k). \quad (2.12)$$

For model A with $E = 0$ these are,

$$T_{mr}^A = \exp(-i\tau m^2/2) \times \left[\frac{2(-i)^{|m-r|}}{\sqrt{1+k^2}} \left(\frac{1 - \sqrt{1+k^2}}{k} \right)^{|m-r|} - \delta_{m,r} \right]. \quad (2.13)$$

The model (2.5) is an Anderson model for localization if the argument of the tangent in (2.7) is replaced by a random variable uniformly distributed in the interval $(0, 2\pi)$. We define a random model AR, corresponding to A by replacing $\frac{1}{2}\tau m^2$ in (2.7) and (2.13) by a sequence of random numbers uniformly distributed in the interval $(0, 2\pi)$. In this case (2.5) is exactly the Lloyd model. In a similar way the model CR is defined as the random model corresponding to C. In what follows the statistics of the quasienergies of the models A and C will be compared with those of the corresponding random models AR and CR respectively. A property of the evolution operator T that is common for all models defined in this section is that it is a band matrix in the angular momentum representation. A band matrix is a matrix where all the large elements lie in a band around its diagonal. The matrix elements T_{mr}^A fall off exponentially with $|m-r|$, the distance from the diagonal (see (2.13)) and those of T_{mr}^C fall off even faster (2.12). This property distinguishes the chaotic systems with time dependent Hamiltonians defined by (1.7) from chaotic systems with time-independent Hamiltonians where all matrix elements can be of the same order of magnitude [10] and therefore the statistics of their energy levels are similar to those predicted by random

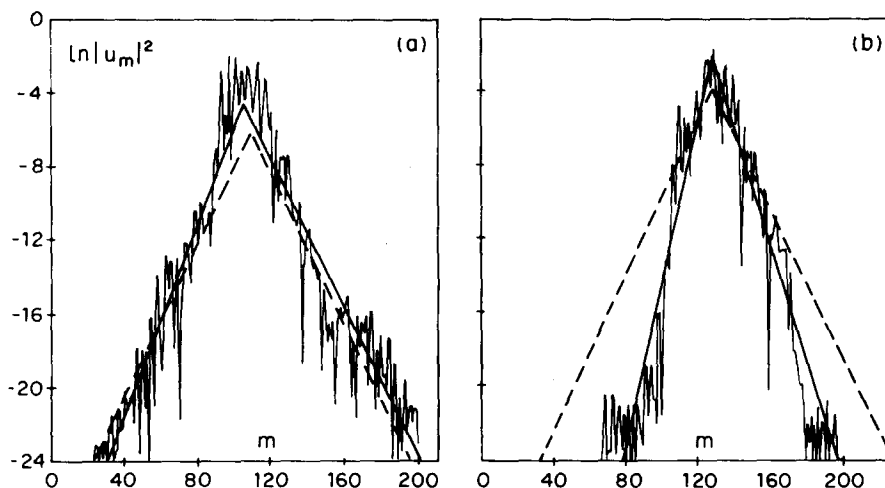


Fig. 1. The amplitude of two quasienergy states of model C as a function of angular momentum for $k=5$ and $\tau=2$. The mean exponential decay of each state is displayed by a heavy line. The average decay for a sample of states is displayed by the dashed line.

matrix theory [10–15]. In this theory it is assumed that the matrix elements satisfy a Gaussian distribution, with the only constraint that it has the same symmetries as the Hamiltonian [1].

The quasienergy states of all these models are exponentially localized in angular momentum i.e. $u_m \sim \exp[-\gamma|m - m_\omega|]$. In fig. 1 two states of model C are presented for $k=5$. The best fit of the averaged localization length $\xi = 1/\gamma$, is $\xi = 9.59 \pm 0.12$. The error results from the fact that the average was performed over a finite number of eigenstates. These eigenstates have different localization lengths and even somewhat different shapes as is obvious from fig. 1. The resulting standard deviation of the localization length is $\sigma_\xi = 5.44$. Note that the states are localized although $k > \pi$. For the corresponding random model CR we find for $k=5$, $\xi = 7.48 \pm 0.08$ and $\sigma_\xi = 4.09$. Although for both models the states are localized the localization lengths are different [34]. In what follows we will be interested to compare between various results of models C and A with comparable localization lengths. For model A we find for $k=9$, $\xi = 8.91 \pm 0.26$ and $\sigma_\xi = 6.44$. This is equal, within the numerical error, to the averaged localization length of the model AR for $k=9$, that is found from (2.11) to be $\xi = 9.02$. The averaged localiza-

tion length of model A is equal to the one of AR (that is equal to the one of the Lloyd model) also for other values of k [25]. Note also that the fluctuation in ξ is of the same order of magnitude as ξ itself. (See also ref. 30.)

3. The distribution of quasienergy separations

The evolution operator T is represented by an infinite matrix in the angular momentum representation. The matrix elements are given explicitly in section 2 for the various models studied in this work (see (2.12) and (2.13)). In order to diagonalize numerically the matrix it was divided into 200×200 non-overlapping blocks having a common diagonal with T . These blocks were diagonalized separately. The matrix T is a band matrix and its eigenstates are exponentially localized. Consequently states that are localized far away from edges of the blocks compared with the localization length are calculated accurately. Only such states are selected for the statistics described in this work. The numerical details of this selection will be described at the end of this section. In fig. 2 we present the distribution of quasienergy separations within such a block. It is approximately a

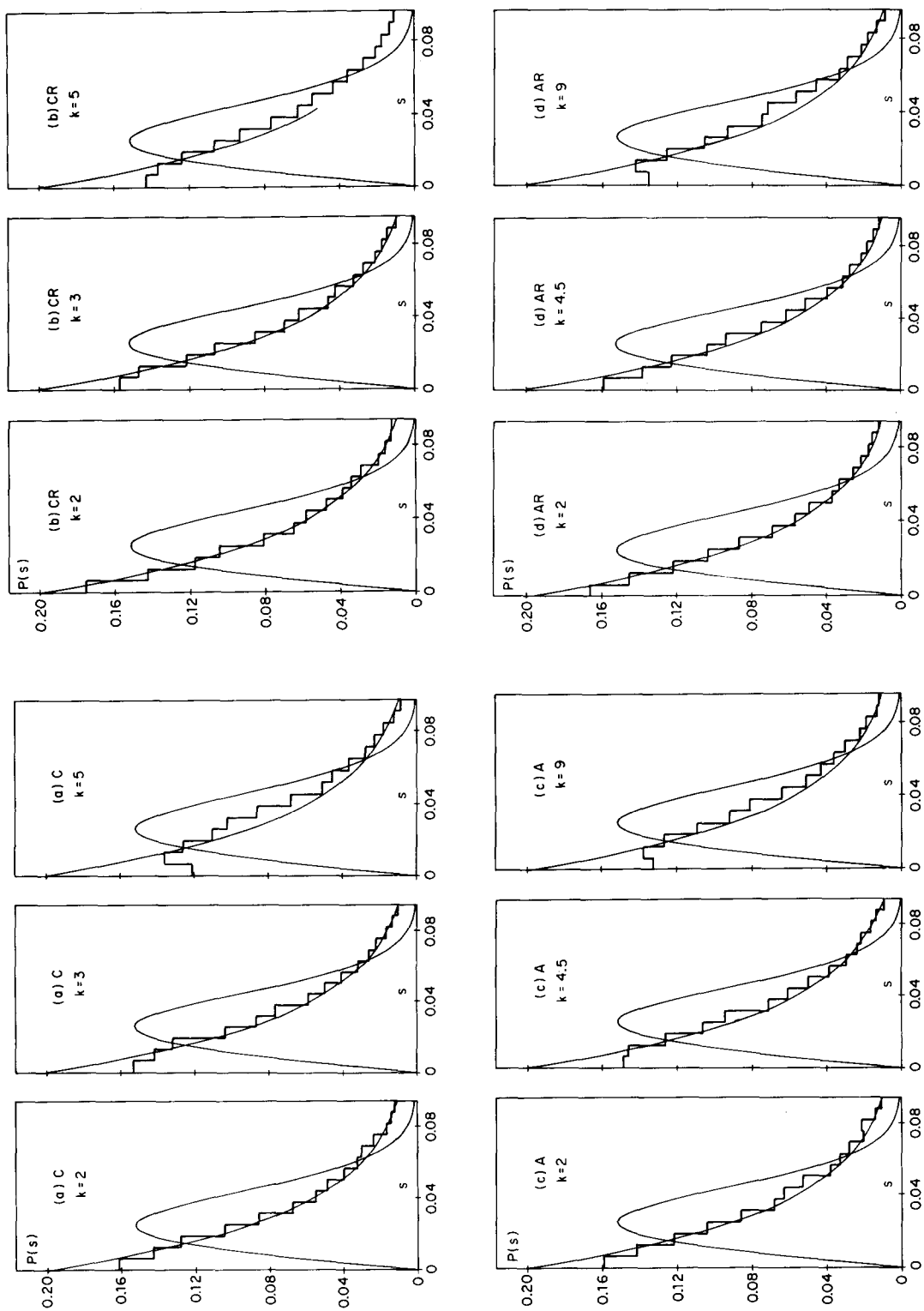


Fig. 2. The distribution $P(s)$ of quasienergy separations in a block for models a) C; b) CR; c) A; d) AR. The values of k are denoted on the figure and $\tau = 2$ for models C and A. The Poisson (1.2) and Wigner (1.1) distributions with the corresponding values of D are plotted for comparison.

Poisson distribution for all models defined in section 2 as expected from localization theory. One can see however that as k increases the deviations from the Poisson distribution increase. This results from the finiteness of the block. As k increases the localization length grows and consequently a larger fraction of the quasienergies repel each other, since they are localized at momentum states that are separated by distances of the order of the localization length or smaller. In the infinite matrix T this fraction vanishes and one expects to obtain a Poisson distribution.

Since the quasienergy spectrum is dense one is forced to study a local spectrum of some type. The quasienergies of finite blocks form a local spectrum determined by the truncation to the block size. In earlier work [27] a local spectrum was obtained for families of quasienergies. The analysis that was performed there for the model C kicked rotor will be extended to all the other models that were defined in section 2. Families F_m^N are formed from quasienergy states that are localized in an interval of length N in angular momentum space, on m states with equal spacing N/m . For this purpose we define a quasienergy state to be localized on a certain angular momentum state if its wave function is maximal for that angular momentum. This is obviously an approximate concept due to strong fluctuations of the wavefunctions as it can be seen in fig. 1. Therefore, on some momenta two quasienergy states or more are localized while on some no such state is localized. Consequently following their definition the families F_m^N can contain a variable number of states. In our previous work families with m , $m - 1$ or $m + 1$ states were used for the analysis of the separations in model C. Each family F_m^N was ordered in quasienergy ω and the separations between the adjacent quasienergies were calculated. The results that were obtained for various families were accumulated, leading to the distribution of the quasienergy separations. It was found that the repulsion of quasienergies increases with k , and a dip at zero in the distribution of the separations develops. This was interpreted as a

result of the general increase of the localization length with k . For fixed N as ξ increases a larger fraction of quasienergies is strongly coupled and therefore repelled. A similar tendency was found also for all the other models that were introduced in this work. In fig. 3 we display the distribution of the quasienergy separations $\tilde{P}(s)$ for various models introduced in the present work. We take $m = 7$ and keep k , and therefore ξ fixed, for each model. All these models share the common feature that the repulsion decreases with N . The reason is that for fixed ξ the fraction of quasienergies with large overlap among themselves decreases with N (for model C it was reported in ref. 27). In particular we find that for models C and A the behavior of $\tilde{P}(s)$ is qualitatively similar. Moreover, it is similar to the behavior of their random counterparts CR and AR. This similarity is expected if it is assumed that Anderson localization takes place for all these models. For models C and CR (figs. 3a and 3b) the strength of the driving is $k = 3$ while for A and AR (figs. 3c and 3d) it is $k = 4.5$. For all these models the localization length is approximately equal and takes the value $\xi \approx 4.5$. This enables one to compare $\tilde{P}(s)$ found for the various models. It depends mainly on the localization length. When $N \gg \xi$ one expects to find nearly no repulsion and indeed for $N = 91$, where $N/2\xi \approx 10$ it is found that $\tilde{P}(s)$ is very close to a Poisson distribution. The deviations of the calculated distribution $\tilde{P}(s)$ from the Poisson distribution with the same mean spacing D are much larger than expected from purely statistical fluctuations (as in ref. 18). For the sake of a quantitative comparison we define $\tilde{\chi}^2 = \chi^2/\chi_s^2$, where χ^2 is the weighted square deviation of $\tilde{P}(s)$ from the Poisson distribution, and χ_s^2 is the mean value that χ^2 would take if the deviations would result only from statistical fluctuations. The weight of each bin in the calculation of χ^2 and χ_s^2 is the inverse of the variance of the number of separations in this bin, if the fluctuations were purely statistical. Therefore $\chi_s^2 + 1$ is equal to the number of bins, namely 15, in our calculation. We found that $\tilde{\chi}_C^2 = 16.69$ and $\tilde{\chi}_A^2 = 13.97$ for the

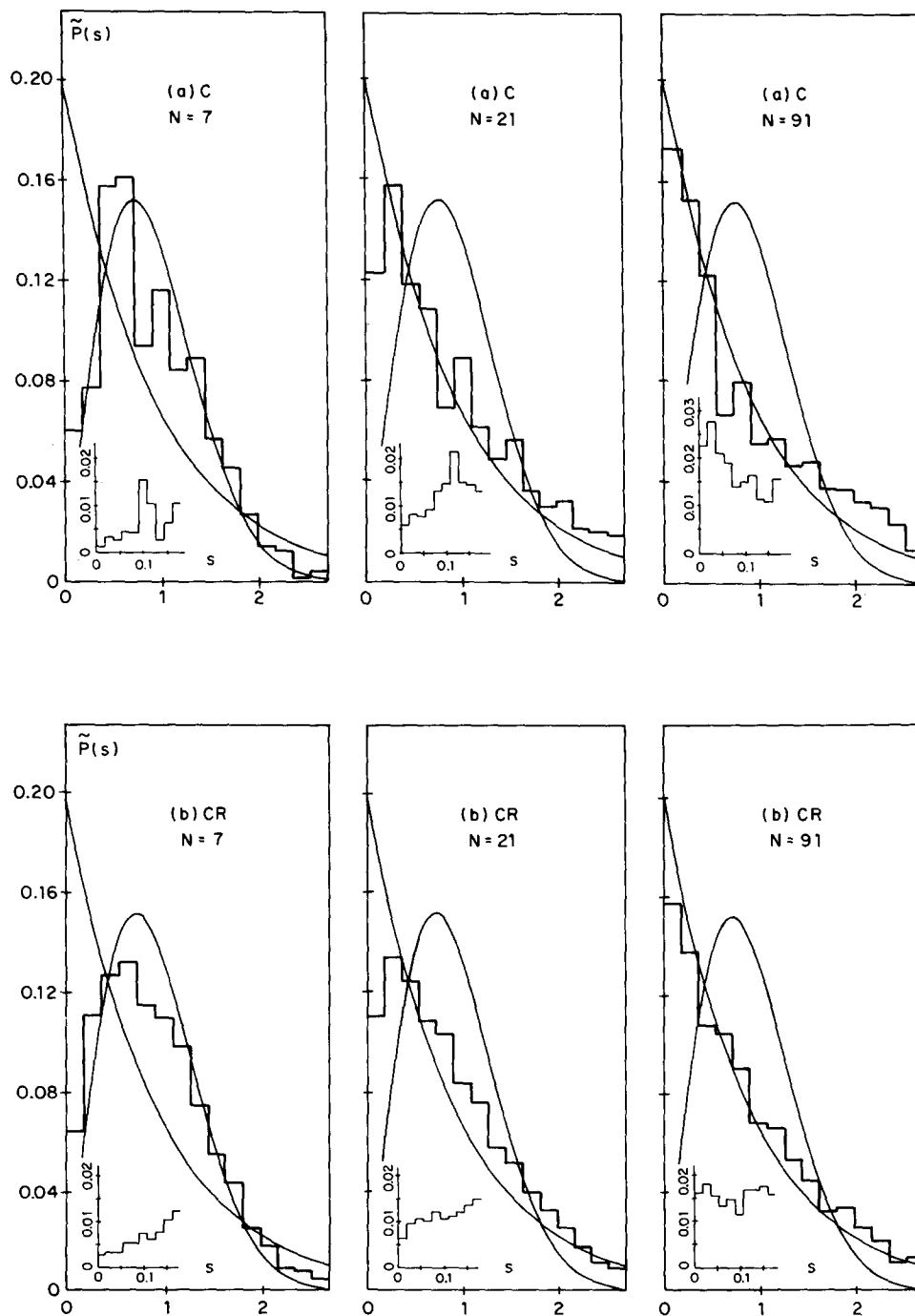


Fig. 3. The distribution of quasienergy spacings $\tilde{P}(s)$ within families, for a) model C, $k = 3$, $\tau = 2$; b) model CR, $k = 3$; c) model A, $k = 4.5$, $\tau = 2$; d) model AR, $k = 4.5$. The Poisson and Wigner distributions are displayed for comparison. The distribution within the first bin is depicted in the insert.

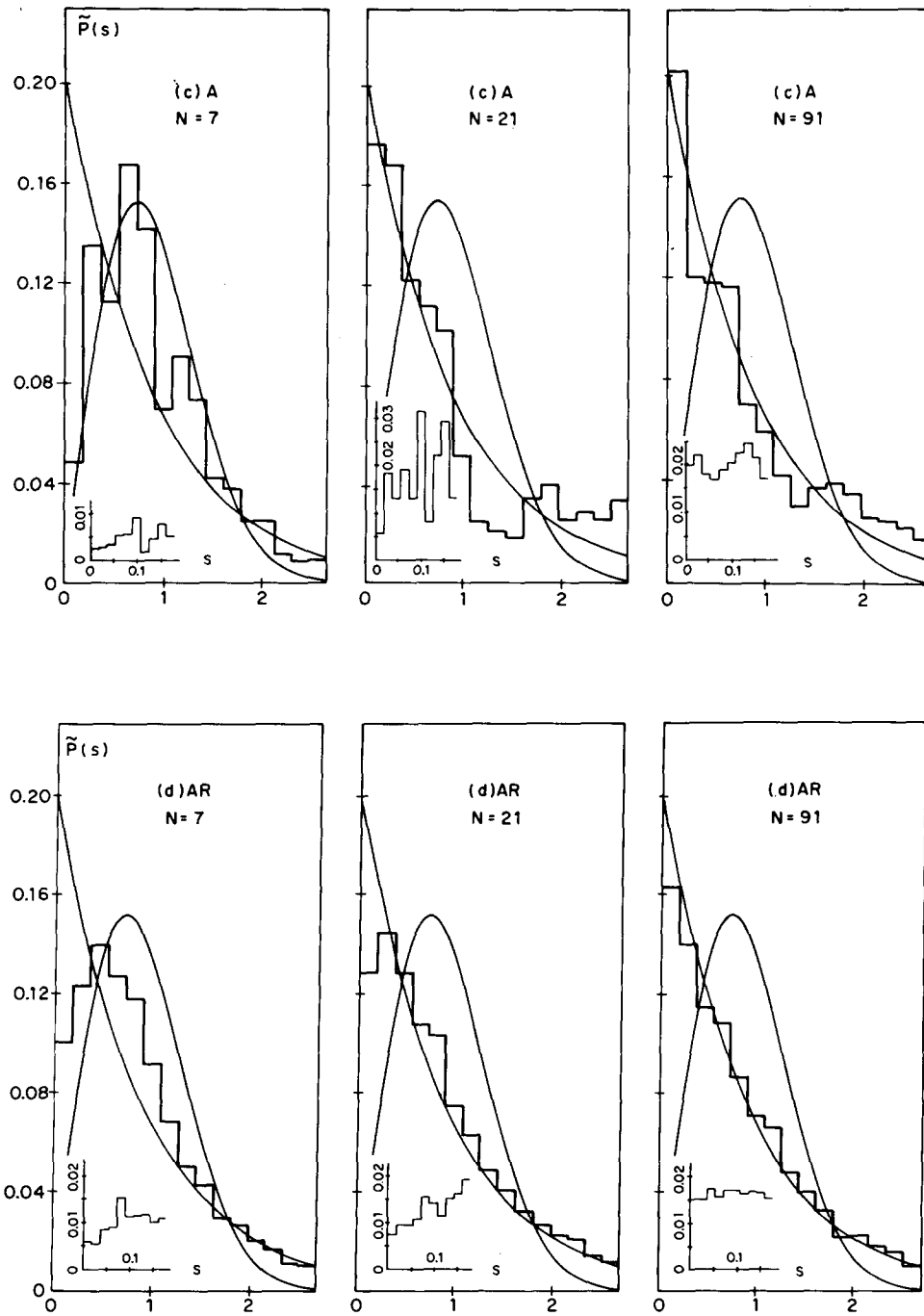


Fig. 3. continued.

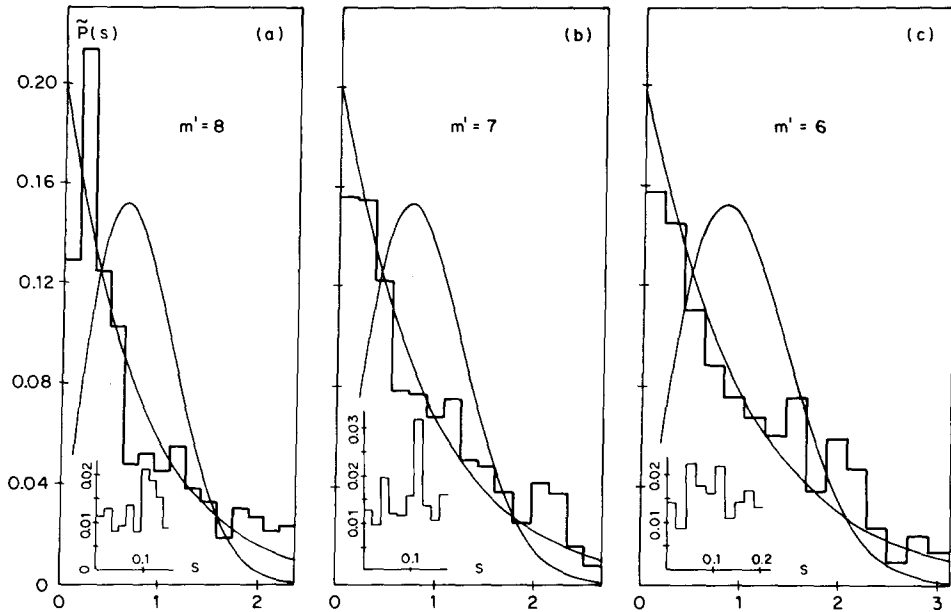


Fig. 4. The distribution $\tilde{P}(s)$ of model C with $k = 3$, $\tau = 2$, $N = 42$, $m = 7$ and a) $m' = 8$; b) $m' = 7$; c) $m' = 6$.

pseudorandom models C and A while $\tilde{\chi}_{\text{CR}}^2 = 6.54$ and $\tilde{\chi}_{\text{AR}}^2 = 2.58$ for the corresponding random models. It is clear that for the pseudorandom models the deviation of $\tilde{P}(s)$ from the Poissonian distribution is considerably larger (for most values of s) than for the corresponding random models. Consequently $\tilde{P}(s)$ that was found for the random models CR and AR is smoother than that of the pseudorandom ones (C, A), as is obvious from fig. 3.

The repulsion depends on the number of levels that are localized on m sites. In the analysis presented in fig. 3 only families consisting of exactly m states were taken into account. For families containing m' quasienergies, with m' that is not necessarily equal to m it is expected that the repulsion increases with m' . In fig. 4 the distribution of separations $\tilde{P}(s)$ is plotted for the model C with $k = 3$, $N = 42$, $m = 7$ and $m' = m + 1$, m and $m - 1$ and indeed such a trend is found. For the other models a similar behavior was found in agreement with expectations. Because of the systematic dependence of $\tilde{P}(s)$ on m' we have taken

into account only families with $m' = m$ in the analysis presented in fig. 3.

We conclude this section with some details of the numerical calculations. As was mentioned, the matrix T was truncated into 200×200 blocks around the diagonal. Due to localization one expects that the states localized inside each block will be calculated accurately and numerical errors will occur for states localized on the edges of the blocks. The matrix T is unitary, therefore the absolute value of all its eigenvalues Λ_ω should satisfy $|\Lambda_\omega| = 1$. At the edges, the unitarity is destroyed and consequently the calculated $|\Lambda_\omega|$ differ from unity. Therefore an eigenvalue Λ_ω of a block is identified as an incorrect one if $||\Lambda_\omega|^2 - 1| > \epsilon$. We checked for some cases that indeed these eigenvalues correspond to states that are localized on the edges of the blocks. The diagonalization of the blocks was performed using the IMSL routine EIGCC. In order to check the routine, τm^2 was replaced by τm in the matrix T (eq. (2.12)) of model C. This becomes an exactly solvable incommensurate model [35]. We found

indeed good agreement with the exact solution of eigenvectors corresponding to eigenvalues satisfying $||\Lambda_\omega|^2 - 1| < \epsilon$. Throughout the calculations of this section the allowed error in the quasienergies was $\epsilon = 0.0083$ which is approximately half the smallest bin in the insert of figs. 3 and 4. The size of this bin is $1/50$ of the mean separation. The results do not change qualitatively with small variations in ϵ . The differences involving wrong eigenvalues are eliminated after the assignment of the eigenvalues to the families F_m^N . This avoids introduction of a bias in the statistics by the elimination. The quasienergy separations are calculated mod 2π namely as angles on a circle. The statistics are such that each of the histograms in fig. 3 contains 3900 differences, while each of the histograms of fig. 4 contains 2900 differences. The size of each bin in the histograms is $D/5$ where D is mean quasienergy spacing. The distribution within the first bin is displayed in the inserts with the bin size of $D/50$. We set $\tau = 2$ in all the numerical calculations for models C and A. The distributions $P(s)$ and $\tilde{P}(s)$ are normalized to be the probabilities to find a separation in the bin that includes s .

4. The Δ_3 -statistic

The Δ_3 -statistic measures the departure of the spectrum from uniformity. From its definition (1.3) it follows that it is a two-point function and therefore it is expected to serve as a useful measure of correlations in the spectrum. In this section it will be evaluated for the models that were defined in section 2. Performing the minimization in (1.3) yields

$$\Delta_3(r) = \left\langle \frac{1}{rD} \int_0^{2L} N(E)^2 dE - 12 \left[\frac{1}{(rD)^2} \int_0^{2L} N(E) E dE \right]^2 - 4 \left[\frac{1}{rD} \int_0^{2L} N(E) dE \right]^2 + 12 \frac{1}{(rD)^3} \int_0^{2L} N(E) E dE \times \int_0^{2L} N(E) dE \right\rangle. \quad (4.1)$$

Using the definition (4.1) it can be transformed by

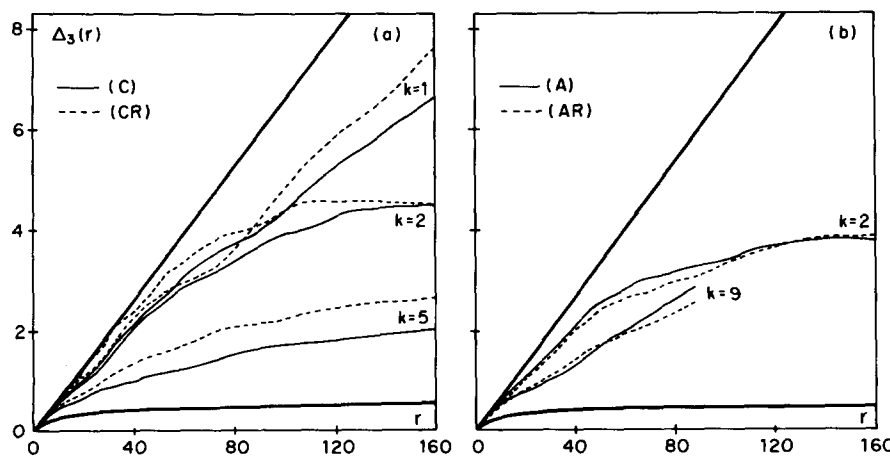


Fig. 5. The statistic $\Delta_3(r)$ for a) models C and CR; b) models A and AR. The heavy lines are the Poisson (1.6) and GOE (1.5) values.

straightforward algebra into a form convenient for numerical calculations, namely,

$$\Delta_3(r) = \left\langle -\frac{1}{rD} \sum_{i=1}^R (2i-1)E_i + \frac{2R}{rD} \sum_{i=1}^R E_i - \frac{4}{(rD)^2} \left[\sum_{i=1}^R E_i \right]^2 - \frac{3}{(rD)^4} \left[\sum_{i=1}^R E_i^2 \right]^2 + \frac{6}{(rD)^3} \left[\sum_{i=1}^R E_i^2 \right] \cdot \left[\sum_{i=1}^R E_i \right] \right\rangle. \quad (4.2)$$

The brackets denote the average over an ensemble of sequences of R levels $\{E_i\}_{i=1}^R$ (R may differ for various sequences). The mean spacing of the levels is D and r is approximately the average number of levels in a sequence, defined as $r = 2L/D$.

The Δ_3 -statistic was computed for the various models defined in section 2 using (4.2). The matrix is divided into blocks and each block is diagonalized separately as described in section 3. The sums in this formula are taken over the sequence of quasienergies in a single block. The ensemble average is performed by averaging the results over various blocks. The resulting values of $\Delta_3(r)$ are presented in fig. 5, for an ensemble of 110 blocks. The values obtained for the pseudorandom models C and A are very close to those of the corresponding random models CR and AR. This is an additional similarity between the random (CR, AR) and the pseudorandom (C, A) models. The values of Δ_3 differ from those of a pure Poisson distribution and the deviation increases with r as is obvious from fig. 5. This deviation will be investigated in some detail in what follows. In the calculation of Δ_3 we used $\varepsilon = 0.1$ rather than the much smaller value that was used in the previous section. The reason is that Δ_3 is not so sensitive as $\tilde{P}(s)$ to the values of the individual eigenvalues. In this way the fraction of eigenvalues that were eliminated was reduced. The plot in fig. 5 terminates at $r = 80$ for models A and AR for $k = 9$ due to elimination of eigenvalues with insufficient accuracy. Because of computer time

limitations Δ_3 was not calculated for $k = 1$ for A and AR models. The deviation of Δ_3 from the behavior of a Poisson distribution is common for all the models that are analyzed in this work and is of a similar nature. It is rigorously established [28] that the energy (E) spectra of models like (2.5) exhibit Poisson distributions. The reason is that energies of states that are exponentially localized far away do not repel each other. This argument should hold also for the quasienergies of the model AR. We found however that its Δ_3 deviates significantly from the Δ_3 of the Poisson distribution, and its deviations are similar to those of the other models. This deviation increases with r . For large k , Δ_3 tends to saturate at a constant value rather than increasing linearly as for a Poisson distribution. This behavior of Δ_3 is understood in the framework of the localization picture. For small r the contributions to Δ_3 arise from quasienergies with small separations. Such quasienergies are not repelled and therefore they belong to states that are localized on momenta that are separated by distances that are large in comparison with the localization length. Such states are to a good approximation statistically independent and consequently satisfy a Poisson distribution. Therefore for small r the statistic Δ_3 is close to its Poissonian value. When r is increased there is a considerable contribution from states that are repelled. Such states are localized on nearby momenta, namely those that are in an interval of the order of the localization length and therefore these are correlated. For any given quasienergy the fraction of quasienergies it repels vanishes for the infinite matrix, but is finite for any finite block. Since the size of blocks that we can diagonalize is limited we introduced a simulation model that demonstrates this effect and displays the gross features exhibited by Δ_3 of the models that were investigated in this work.

The simulation model (SM) consists of \tilde{N} quasienergies divided into $M = \tilde{N}/\tilde{\xi}$ families. Each family consists of $\tilde{\xi}$ quasienergies with equal spacing $D = 2\pi/\tilde{\xi}$. The various M families are totally uncorrelated. The family size $\tilde{\xi}$ is a parameter of

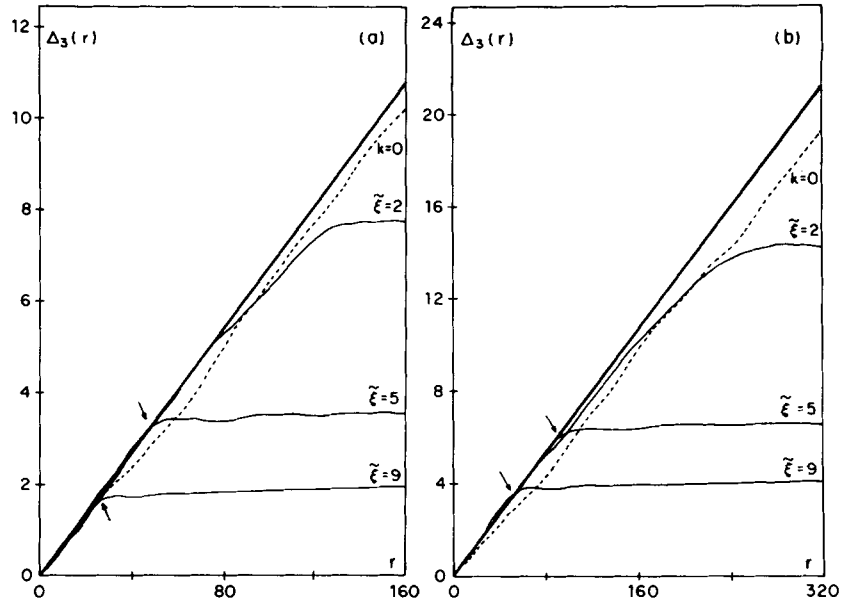


Fig. 6. The statistic $\Delta_3(r)$ for the simulation model—(continuous lines), decoupled ($k=0$) model C (dashed line) and Poisson distribution (heavy line). The number of quasienergies is a) $\tilde{N} = 200$, b) $\tilde{N} = 400$. The arrow marks r^* .

the model and simulates the localization length. The Δ_3 of this model for $\tilde{N} = 200$ is displayed in fig. 6a for various values of $\tilde{\xi}$ that are approximately equal to values of ξ for which the other models were analyzed. In the SM there is a Poisson like behavior for small r , namely, $\Delta_3(r)$ is a straight line with a slope of $1/15$. For large r it approaches $\Delta_3(r) = \text{const}$. Such behavior characterizes the equally spaced spectrum as can easily be seen substituting $E_i = Di$ in (4.2) leading to (see also ref. 4)

$$\Delta_3(r) = \frac{1}{12}(1 - r^{-2}). \quad (4.3)$$

For large $\tilde{\xi}$ the crossover between the two regimes is a well-defined point r^* . The sharp crossover results from the special property of the SM that quasienergies are either totally uncorrelated or exactly equally spaced. For the other models this crossover is smooth. In both cases Δ_3 saturates at a constant value as is clear from comparison between fig. 5 and fig. 6a. For large $\tilde{\xi}$ there is even quantitative agreement and the value found for $\tilde{\xi} = 9$ in the SM is close to the one obtained for the

C and CR models with $\xi \approx 9$. From fig. 6a we note also that for $k=0$ where the quasienergies are just $(\frac{1}{2}\pi m^2) \bmod 2\pi$, Δ_3 is close to its value for a Poisson distribution.

The comparison between fig. 5 and fig. 6a leads us to believe that the SM accounts for the main cause for the deviation from the Poisson distribution. Therefore we study the effect of block finiteness in the framework of this model. For this purpose Δ_3 was calculated for $\tilde{N} = 400$ and the results are presented in fig. 6b. The plot has a similar form as fig. 6a but with all the scales increased by a factor of two. In particular the crossover point is

$$r^* = \bar{\mu}(\tilde{\xi}) \tilde{N}, \quad (4.4)$$

where $\bar{\mu}(\tilde{\xi})$ is independent of \tilde{N} . For example $\bar{\mu}(\tilde{\xi} = 9) = 0.128$. In general $r^* \approx \tilde{N}/\tilde{\xi}$, since for $r < \tilde{N}/\tilde{\xi}$ mainly quasienergies belonging to different families contribute to Δ_3 , while for $r > \tilde{N}/\tilde{\xi}$ also quasienergies that belong to the same family must contribute to Δ_3 . Consequently, $\bar{\mu}(\tilde{\xi}) \approx 1/\tilde{\xi}$. This implies that $r^* \rightarrow \infty$ in the limit $\tilde{N} \rightarrow \infty$. In

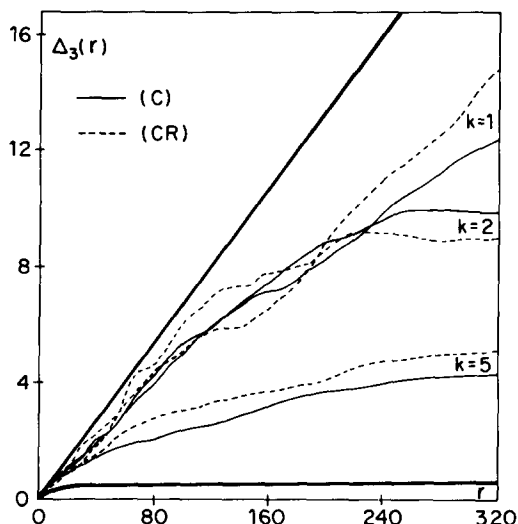


Fig. 7. Same as fig. 5a but with sums in (4.2) over pairs of blocks.

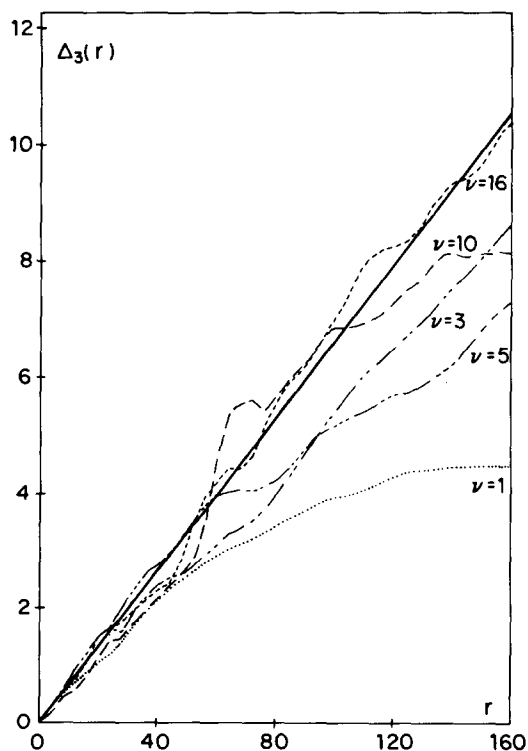


Fig. 8. The statistic $\Delta_3(r)$ of model C for $k=2$, summing over ν blocks.

fig. 7 the statistic Δ_3 is displayed but the sums in (4.2) are over quasienergies belonging to pairs of blocks. The ensemble contains 55 independent pairs. Comparison with fig. 5 reveals a scaling similar to the one found for the SM. We repeated the calculation of Δ_3 taking the sums in (4.2) over quasienergies of ν blocks and the ensemble average over $110/\nu$ groups of blocks. The results are shown in fig. 8 for model C with $k=2$. The Poissonian behavior is approached as ν increases. This regrouping of blocks is in some sense similar to the increase of the block size. This scaling of Δ_3 with the block size leads us to believe that it approaches true Poissonian behavior in the limit of the infinite T matrix.

5. Conclusions

In the present work it was demonstrated that the statistics of quasienergies for various systems, with time dependent Hamiltonians, are similar to those of models for localization of electrons in disordered solids. This provides further evidence for Anderson localization in certain dynamical systems, with time-dependent Hamiltonians, such as (1.7). This is in agreement with earlier work, where the correspondence between these problems was proposed [25]. In particular the spectrum of the quasienergies satisfies Poissonian statistics, as reflected in the distribution of their separations and in the Δ_3 statistic. The deviations from Poissonian statistics, that are found in the numerical calculations are related to the block truncation of the matrix of the evolution operator. Although the kicked rotor is chaotic in the classical limit, the statistics of its quasienergies are very different from those found so far, for systems with time independent Hamiltonians. These statistics result from Anderson localization in angular momentum, that takes place for the kicked rotor. Quasienergies that are localized in angular momentum within distances of the order of the localization length or smaller are repelled. In this work we studied two pseudorandom models, defined by the

Hamiltonian (1.7), as well as two truly random models. A remarkable, detailed and quantitative similarity between the statistics of the quasienergies of these models was found. These are determined primarily by the localization length. Therefore we conclude that the behavior of these systems is controlled mainly by Anderson localization. There are, however, differences in quantitative details between the pseudorandom and the corresponding random models. Such differences are, for example, the deviation from the Poisson distribution for finite systems (section 3) and the value of the localization length (section 2 and ref. 34). Differences of this nature should be investigated in detail in further studies.

Acknowledgements

We thank D.R. Grempel, N. Moiseyev and R.E. Prange for useful suggestions and comments. The work was supported in part by the U.S.-Israel Binational Science Foundation (BSF), by the Bat-Sheva de-Rothschild Fund for Advancement of Science and Technology and by the Technion VPR-L. Deutsch Research Fund.

References

- [1] M.L. Mehta, *Random Matrices and Statistical Theory of Energy Levels* (Academic, New York, 1967); *Statistical Theories of Spectra; Fluctuations*, C.E. Porter, ed. (Academic, New York, 1965). M. Carmeli, *Statistical Theory and Random Matrices* (Dekker, New York, 1983).
- [2] T.A. Brody, J. Flores, J.B. French, P.A. Mello, A. Pandey and S.S.H. Wong, *Rev. Mod. Phys.* 53 (1981) 385.
- [3] N. Rosen, Z. Weig and C.E. Porter, *Phys. Rev.* 120 (1960) 1698.
- [4] E. Haller, H. Koppel and L.S. Cederbaum, *Chem. Phys. Lett.* 101 (1983) 215.
- [5] F.J. Dyson and M.L. Mehta, *J. Math. Phys.* 4 (1963) 701.
- [6] For a review see e.g. E. Ott, *Rev. Mod. Phys.* 53 (1981) 655.
- [7] A.J. Lichtenberg and M.A. Leiberman, *Regular and Stochastic Motion* (Springer, Berlin, 1983). H.G. Schuster, *Deterministic Chaos* (Physik-Verlag, Weinheim, 1984).
- [8] M.V. Berry, in: *Chaotic Behavior of Deterministic Systems*, Proc. Les-Houches Summer School, G. Iooss, R.H.G. Helleman and R. Stora, eds. (North-Holland, Amsterdam, 1983).
- [9] G. Zaslavsky, *Phys. Repts.* 80 (1981) 158.
- [10] P. Pechukas, *Phys. Rev. Lett.* 51 (1983) 943.
- [11] M.V. Berry, *Ann. Phys. (NY)* 131 (1981) 163.
- [12] M.V. Berry and M. Tabor, *Proc. Roy. Soc. Lond. A* 356 (1972) 375.
- [13] O. Bohigas, M.J. Giannoni and C. Schmit, *Phys. Rev. Lett.* 52 (1984) 1. S.W. McDonald and A.N. Kaufman, *Phys. Rev. Lett.* 42 (1979) 1189. G. Casati, F. Valz-Gris and I. Guarneri, *Nuovo Cimento Lett.* 28 (1980) 279.
- [14] E. Haller, H. Koppel and L.S. Cederbaum, *Phys. Rev. Lett.* 52 (1984) 1665. T.H. Seligman, J.J.M. Verbaarschot and M.R. Zirnbauer, *Phys. Rev. Lett.* 53 (1984) 215.
- [15] M. Feingold, N. Moiseyev and A. Peres, *Phys. Rev. A* 30 (1984) 509.
- [16] M. Shapiro and G. Goelman, *Phys. Rev. Lett.* 53 (1984) 1714.
- [17] M.V. Berry and M. Robnick, *J. Phys. A* 17 (1984) 2413.
- [18] G. Casati, B.V. Chirikov and I. Guarneri, *Phys. Rev. Lett.* 54 (1985) 1350.
- [19] M. Feingold, *Phys. Rev. Lett.* 55 (1985) 2626.
- [20] M.V. Berry, *Proc. Roy. Soc. A* 400 (1985) 229.
- [21] B.V. Chirikov, *Phys. Rep.* 52 (1979) 263.
- [22] G. Casati, B.V. Chirikov, F.M. Izrailev and J. Ford, in: *Stochastic Behavior in Classical and Quantum Hamiltonian Systems*, G. Casati and J. Ford, eds., *Lecture Notes in Physics*, vol. 93 (Springer, Berlin, 1979).
- [23] B.V. Chirikov, F.M. Izrailev and D.L. Shepelyansky, *Sov. Sci. Rev. Sec. C* 2 (1981) 209.
- [24] T. Hogg and B. Huberman, *Phys. Rev. Lett.* 48 (1982) 711; *Phys. Rev. A* 28 (1983) 22.
- [25] S. Fishman, D.R. Grempel and R.E. Prange, *Phys. Rev. Lett.* 49 (1982) 509; D.R. Grempel, R.E. Prange and S. Fishman, *Phys. Rev. A* 29 (1984) 1639; R.E. Prange, D.R. Grempel and S. Fishman, in: *Chaotic Behavior in Quantum Systems*, Proc. Como Conference on Quantum Chaos, G. Casati, ed. (Plenum, New York, 1984).
- [26] For a review see e.g. D.J. Thouless, in: *Ill Condensed Matter*, Proc. Les Houches Summer School, vol. 31, R. Balian, R. Maynard and G. Toulouse, eds. (North-Holland, Amsterdam, 1979). P.A. Lee and T.V. Ramakrishnan, *Rev. Mod. Phys.* 57 (1985) 287.
- [27] M. Feingold, S. Fishman, D.R. Grempel and R.E. Prange, *Phys. Rev. B* 31 (1985) 6852.
- [28] S.A. Molcanov, *Commun. Math. Phys.* 78 (1981) 429.
- [29] F.M. Izrailev, *Phys. Rev. Lett.* 56 (1986) 541.
- [30] D.L. Shepelyansky, *Phys. Rev. Lett.* 56 (1986) 677.
- [31] P. Lloyd, *J. Phys. C* 2 (1969) 1717.
- [32] D.J. Thouless, *J. Phys. C* 5 (1972) 77.
- [33] K. Ishii, *Prog. Theor. Phys., Suppl.* 53 (1973) 77.
- [34] For a more complete investigation of this point see: R. Blumel, S. Fishman, M. Griniasti and U. Smilansky, to be published in Proc. 2nd Int. Conf. Quantum Chaos, Cuernavaca, Mexico, Jan. 1986.
- [35] D.R. Grempel, S. Fishman and R.E. Prange, *Phys. Rev. Lett.* 49 (1982) 833; R.E. Prange, D.R. Grempel and S. Fishman, *Phys. Rev. B* 29 (1984) 6500.